# Analysis of Dust Retention Capacity in Typical Plant Communities Along Roadside Green Belts in Southern Xinjiang During Spring and Summer

Fei Wang , Jun Yu * , Ruiheng Lv * , Fengzhen Chang

Posted Date: 9 February 2026

doi: 10.20944/preprints202602.0618.v1

Keywords: urban roadside green spaces; plant communities; dust retention capacity; leaf surface microstructure; arid environment; southern Xinjiang

 doi:10.20944/preprints202602.0618.v1



*Article*

# Analysis of Dust Retention Capacity in Typical Plant Communities Along Roadside Green Belts in Southern Xinjiang During Spring and Summer

**Fei Wang [1], Jun Yu [1,*], Ruiheng Lv [1,*] and Fengzhen Chang [2]**

[1] College of Horticulture and Forestry, Tarim University, Alaer 843300,China

[2] College of Hydraulic and Architectural Engineering, Tarim University, Alaer 843300, China

* Correspondence: 119920014 @taru.edu.cn (J.Y.); 120100063@taru.edu.cn (R.L.)

**Abstract**

Roadside green spaces function as critical ecological barriers in urban environments, and their plant communities play a key role in improving regional air quality. This study investigates typical roadside plant communities in southern Xinjiang, a region characterized by extreme aridity and frequent dust storms. By quantifying indicators such as dust retention capacity at both individual and community levels, together with leaf surface microstructural characteristics, we evaluate the comprehensive dust retention performance of different community configuration patterns. The results show that: (1) Among the studied species, *Juniperus chinensis 'Kaizuca'* exhibited the highest dust retention capacity per unit leaf area, followed by *Juniperus chinensis L.* and *Rosa rugosa Thunb*. Among trees, *Platanus acerifolia (Aiton) Willd* showed the greatest dust retention capacity per individual plant; among shrubs, *Rosa rugosa Thunb*. performed strongly; and among herbaceous species, *Lolium perenne L.* exhibited relatively high dust retention capacity. (2) Leaf dust retention is governed by the synergistic effects of multiple traits, including leaf aspect ratio, stomatal aspect ratio, stomatal protrusion, stomatal density, wax layer characteristics, and surface roughness. Leaf aspect ratio exerts a significant positive direct effect on dust retention, whereas stomatal aspect ratio shows a significant negative direct effect. (3) At the community level, the multi-layered tree–shrub–herbaceous configuration dominated by *Platanus acerifolia (Aiton) Willd* exhibited the strongest dust retention capacity, making it the most effective configuration for roadside green spaces. Overall, this study provides a robust theoretical framework and empirical evidence for the scientific selection and optimized configuration of roadside vegetation in arid regions, thereby supporting the sustainable improvement of urban roadside air quality in southern Xinjiang.

**Keywords:** urban roadside green spaces; plant communities; dust retention capacity; leaf surface microstructure; arid environment; southern Xinjiang

## 1. Introduction

Against the backdrop of growing global concern over atmospheric particulate pollution and the rapid expansion of urbanization and industrialization, airborne particulate matter has become a critical environmental issue threatening human health and urban ecosystems [1]. Fine particulate matter can remain suspended in the atmosphere for extended periods, adsorb toxic substances, and penetrate deep into the human respiratory system, thereby inducing respiratory and pulmonary diseases [2]. It significantly increases the incidence of chronic respiratory disorders and cardiovascular conditions such as hypertension [3] , making particulate pollution a central concern in urban atmospheric environments [4]. In arid and semi-arid regions, frequent dust storms further elevate particulate concentrations, posing persistent risks to residents' quality of life and urban air quality [5].

 doi:10.20944/preprints202602.0618.v1



Plant communities provide essential ecological services, including cooling, humidification, and microclimate regulation, while also enhancing recreational spaces and human thermal comfort [6]. Roadside green spaces function as important ecological buffers in cities, and the dust retention capacity of their vegetation represents an effective natural mechanism for mitigating air pollution [7,8]. Previous studies have demonstrated that urban green spaces can substantially reduce airborne particulate concentrations through processes such as adsorption, interception, and deposition [9]. Consequently, the scientific and rational planning of green space structures to suppress dust and improve local air quality has become a key issue in contemporary urban ecological development [10,11].

Southern Xinjiang, located in China's largest inland basin, contains the Taklamakan Desert—the largest desert in China, the world's tenth largest desert, and the second-largest shifting desert globally—at the center of the Tarim Basin. According to the 2024 Xinjiang Ecological Environment Status Bulletin and the National Economic and Social Development Statistical Bulletin, supplemented by data from the National Qinghai–Tibet Plateau Scientific Data Center, air quality in southern Xinjiang reached the "good" level for 88% of the year in 2024. However, days with air quality at or above the "light pollution" level accounted for 12%. Among polluted days, exceedances were dominated by coarse particulate matter ($PM_{10}$), which accounted for 85.5% of all exceedance events. Existing research further indicates that dust storms are a major driver of elevated $PM_{10}$ concentrations in this region [12] . Therefore, dust storms constitute a primary source of atmospheric particulate pollution in urban areas of southern Xinjiang [13].

Extensive research has explored the dust retention capacity of urban vegetation from multiple perspectives, including tree species composition, leaf microstructure, canopy characteristics, community scale, and configuration patterns, providing valuable insights for optimizing urban green space design. For example, studies in Xi'an (annual precipitation 500–690 mm) have shown that plant communities with higher canopy closure exhibit stronger particulate adsorption capacity [14]. Research in the Baramati region of India (annual precipitation ~1000 mm) has identified the Air Pollution Tolerance Index (APTI) as a key determinant of particulate retention potential in roadside vegetation [15]. Similarly, studies in Nanjing (annual precipitation ~1100 mm) have demonstrated that leaf surface roughness and nitrogen content are primary factors driving differences in dust retention among plant species [16]. These findings indicate that existing research on plant dust deposition has largely focused on humid regions with high urbanization levels, where atmospheric particulate matter is dominated by $PM_{2.5}$ and $PM_{10}$. However, the mechanisms governing variations in dust retention capacity under arid climatic conditions—where sand dust interacts with $PM_{2.5}$ and $PM_{10}$—remain insufficiently understood.

In this context, the present study focuses on southern Xinjiang, a region characterized by extreme aridity, fragile ecosystems, and frequent spring dust storms [17]. We quantify the dust retention dynamics of typical roadside plant communities during the main growing season from May to August, with the following objectives: (1) to quantitatively evaluate dust retention capacity across different plant species at the levels of unit leaf area, individual plants, and plant communities; (2) to analyze leaf surface structural characteristics and elucidate the microstructural mechanisms underlying interspecific differences in dust retention capacity; and (3) to identify plant species with high particulate retention potential and optimize community configuration patterns for roadside green spaces.

## 2. Research Area and Methods

### *2.1. Study Area*

Alaer City is located in Aksu Prefecture and is one of the core cities in southern Xinjiang, China (80°35′–81°58′E, 40°22′–40°57′N). The city lies at an average elevation of approximately 1,011 m and is situated at the southern foothills of the Tianshan Mountains and the northern margin of the Tarim Basin (Figure 1). It is located near the confluence of the Yarkant, Hotan, and Aksu rivers in the upper

 doi:10.20944/preprints202602.0618.v1



reaches of the Tarim River. Alaer City borders Shaya County to the east, Awati County to the west, the Taklamakan Desert to the south, and the Tianshan Mountains to the north. The administrative area of Alaer City covers approximately 6,923.4 km². The mean annual temperature is about 10.7 °C. The recorded extreme minimum temperature is −28 °C (with a minimum of −33.2 °C in the Fourth Brigade Reclamation Area), whereas the extreme maximum temperature reaches 35 °C (with temperatures up to 40 °C occurring every 5–10 years in the Shajingzi Reclamation Area). The region is characterized by low precipitation, minimal winter snowfall, and intense surface evaporation. Mean annual precipitation ranges from 40.1 to 82.5 mm, while mean annual evaporation ranges from 1,876.6 to 2,558.9 mm, far exceeding precipitation. Consequently, Alaer City exhibits a typical warm-temperate, extremely continental arid desert climate.

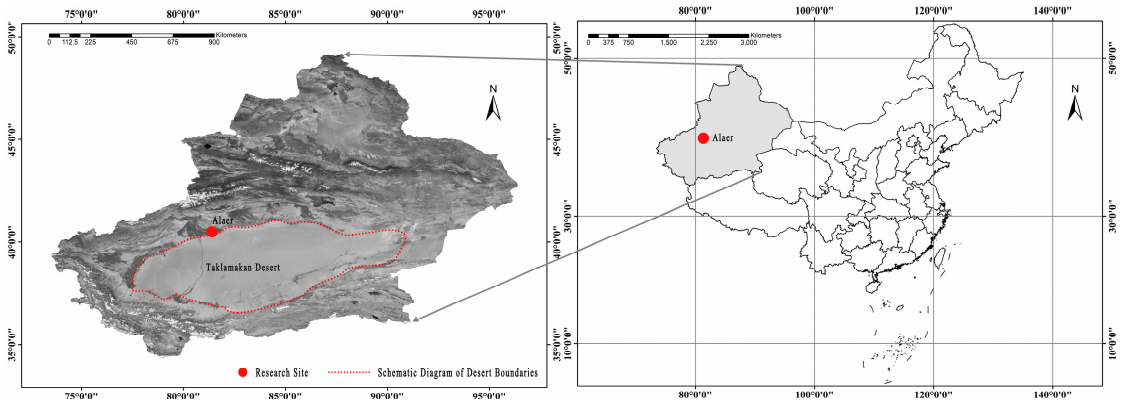


**Figure 1.** Location of the main urban area of Alaer City, Xinjiang.

The study area is adjacent to the Taklamakan Desert and located at the northern edge of the Tarim Basin. Statistical data from Alaer City over the past decade (National Qinghai–Tibet Plateau Science Data Center) indicate that Alaer City has one of the highest average particulate matter concentrations among counties and cities in Xinjiang. Sandstorms occur frequently during spring and summer, particularly from May to August. Based on plant phenology, the experimental period was therefore defined as May–August 2025.

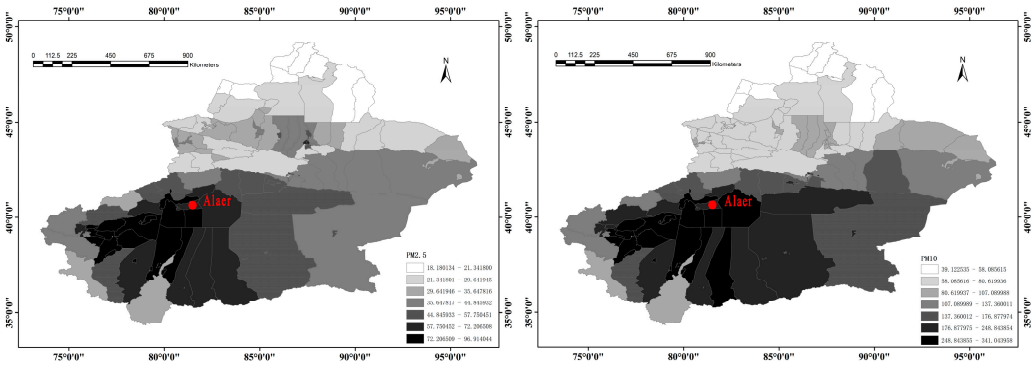


**Figure 2.** Temporal variation in $PM_{2.5}$ and $PM_{10}$ concentrations in Alaer City over the past decade.

*2.2. Plot Selection and Plot Layout*

Based on literature review and field surveys, the dominant tree species in Alaer's urban areas include *Malus spectabilis*, *Fraxinus chinensis*, *Platanus acerifolia*, *Sophora japonica*, *Ulmus pumila*, and *Juniperus chinensis*. The main shrub species include *Juniperus chinensis*, *Platycladus orientalis*, *Ligustrum obtusifolium*, *Ulmus pumila 'Jinye'*, and *Prunus triloba*. Accordingly, this study focused on three representative tree species—*Malus spectabilis (Aiton) Borkh.*, *Fraxinus chinensis Roxb.*, and *Platanus*

 doi:10.20944/preprints202602.0618.v1



*acerifolia (Aiton) Willd*. Four major urban roads (Xingfu Road, Shengli Avenue, Kungang Avenue, and Banchao Avenue) were selected, and eight roadside green spaces representing three vegetation configuration patterns were established as study plots (Table 1). Typical roadside green space configurations in Alaer were selected, excluding extremely small saplings and unusually large old trees. Sample plots of 6 m × 10 m and 7 m × 10 m were established, and sampling was conducted from May to August.

**Table 1.** Information on study plots for dust retention in different plant communities.

| Community Structure | Plot Number | Plot size | Plant Name | Crown density |
|---|---|---|---|---|
| Tree-Shrub-Herbaceous | 1# | 6 m × 10 m | *Malus spectabilis (Aiton) Borkh.*<br>*Ulmus pumila 'Jinye'*<br>*Ligustrum obtusifolium Siebold & Zucc.*<br>*Juniperus chinensis L.*<br>*Poa annua L.* | 0.91 |
| | 2# | 7 m × 10 m | *Malus spectabilis (Aiton) Borkh.*<br>*Rosa rugosa Thunb.*<br>*Lolium perenne L.* | 0.94 |
| | 3# | 6 m × 10 m | *Fraxinus chinensis Roxb.*<br>*Amorpha fruticosa L.*<br>*Lolium perenne L.* | 0.92 |
| | 4# | 7 m × 10 m | *Platanus acerifolia (Aiton) Willd*<br>*Malus spectabilis (Aiton) Borkh.*<br>*Prunus triloba Lindl.*<br>*Ligustrum obtusifolium Siebold & Zucc.*<br>*Rosa chinensis Jacq.*<br>*Poa annua L.* | 0.94 |
| Tree-Shrub | 5# | 6 m × 10 m | *Malus spectabilis (Aiton) Borkh.*<br>*Juniperus chinensis 'Kaizuca'*<br>*Platycladus orientalis (L.) Franco*<br>*Rosa chinensis Jacq.* | 0.87 |
| | 6# | 7 m × 10 m | *Platanus acerifolia (Aiton) Willd*<br>*Malus spectabilis (Aiton) Borkh.*<br>*Juniperus chinensis 'Kaizuca'*<br>*Ulmus pumila 'Jinye'* | 0.93 |
| Tree-Herbaceous | 7# | 6 m × 10 m | *Malus spectabilis (Aiton) Borkh.*<br>*Catalpa speciosa (Warder ex Barney) Engelm.*<br>*Lolium perenne L.* | 0.92 |
| | 8# | 6 m × 10 m | *Fraxinus chinensis Roxb.*<br>*Malus spectabilis (Aiton) Borkh.*<br>*Lolium perenne L.* | 0.91 |

### *2.3. Materials and Methods*

#### 2.3.1. Measurement of Leaf Dust Retention Capacity in Plant Communities

Sampling was conducted from May to August 2025 on clear, rain-free days with calm or weak wind conditions, and all sampling was completed within one day. Based on plant morphology and height within each plot, the canopy was divided into upper, middle, and lower layers for stratified sampling. Nine leaves were collected evenly from the east, south, west, and north directions of each sampled plant. Leaves were placed in polyethylene resealable bags and stored in a cooler for subsequent analysis. Vibration during collection and transportation was minimized to prevent particulate loss from leaf surfaces.

 doi:10.20944/preprints202602.0618.v1



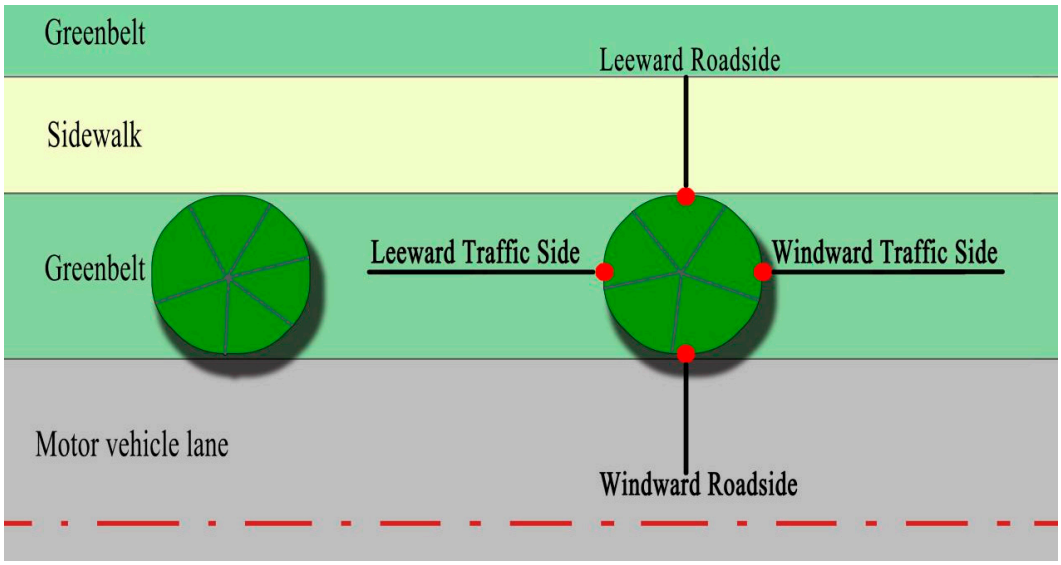


**Figure 3.** Schematic diagram of leaf sampling positions.

Leaf samples were soaked for at least 2 h to remove surface dust and rinsed repeatedly with distilled water until all particulate matter was transferred into the soaking solution [18]. The solution was filtered under vacuum using pre-dried and weighed quantitative filter paper ($M_1$). The filter paper was then dried at 60 °C for 24 h, reweighed, and Surface-Based recorded as $M_2$. Leaf area was determined by scanning leaves and analyzing images using ImageJ software (Fiji, Version 2023.09.25) [19,20] .

Dust retention capacity per unit leaf area was calculated as:

$$X_1 = \frac{M_2 - M_1}{S} \quad (1)$$

Total leaf area per plant was estimated as:

$$R=\exp\{0.6031+0.2375H+0.6906D-0.0123[\pi（H+D)/2)\}+0.1824 \quad (2)$$

Dust retention capacity per plant was calculated as:

$$X_2 = X_1 \times R \quad (3)$$

where $X_1$ is dust retention per unit leaf area (g·m$^{-2}$); $M_1$ and $M_2$ are the masses of filter paper before and after filtration (g); $S$ is leaf area (m$^2$); $R$ is total leaf area per plant; $H$ is crown height; and $D$ is mean crown width.

2.3.2. Scanning Electron Microscopy of Leaf Surface Structure

Fixed leaf samples were sequentially dehydrated in ethanol solutions of 30%, 50%, 70%, 85%, and 95%, followed by two 20-min treatments with absolute ethanol. Samples were then dried using a critical point dryer and sputter-coated with gold. Leaf microstructures were observed using a field-emission scanning electron microscope (Thermo Fisher Scientific, Apreo S, USA). Representative fields of view were selected, and micrographs were obtained [21].

2.3.3. Calculation of Dust Retention Capacity in Roadside Plant Communities

Representative roadside plant communities were selected, and vegetation information within 10 m × 6 m and 10 m × 7 m plots was recorded. Community dust retention capacity per unit area was calculated as the sum of dust retention capacity per individual plant multiplied by the number of individuals of each species, divided by plot area [22] .

 doi:10.20944/preprints202602.0618.v1



2.3.4. Calculation of Community Cooling and Humidification Rates

The cooling rate of plant communities was calculated as:

$$T = \frac{T_s - T_m}{T_s} \times 100\% \quad (4)$$

The humidification rate was calculated as:

$$RH = \frac{RH_s - RH_m}{RH_s} \times 100\% \quad (5)$$

where $T_s$ and $RH_s$ represent temperature and relative humidity at control points outside the green space, and $T_m$ and $RH_m$ represent values measured within the green space.

2.3.5. Comprehensive Evaluation of Community Dust Retention Capacity

Raw data were standardized as:

$$Z = \frac{x_{ij} - \overline{x_{ij}}}{\sigma} \quad (6)$$

The proportion of the i-th community under the j-th indicator was calculated as:

$$p_{ij} = \frac{x_{ij}}{\sum_{i=1}^{m} x_{ij}} \quad (7)$$

The entropy value of indicator j was calculated as:

$$e_j = -k \sum_{i=1}^{m} p_{ij} \ln p_{ij} \quad (8)$$

The coefficient of variation was calculated as:

$$g_j = 1 - e_j \quad (9)$$

The weight of indicator j was calculated as:

$$w_j = \frac{g_j}{\sum_{i=1}^{m} g_j} \quad (10)$$

The comprehensive dust retention capacity score for community i was calculated as:

$$S_i = \sum_{j=1}^{n} w_j \, x_{ij} \quad (11)$$

Higher indicator weights indicate greater contributions to the overall evaluation, and higher composite scores represent stronger dust retention capacity performance of plant communities [23].

2.3.6. Statistical Analysis

Statistical analyses were performed using Excel 2014 (Microsoft Corp., Redmond, WA, USA) and SPSS 27 (IBM, Armonk, NY, USA). Differences in dust retention capacity among plant communities were assessed using LSD multiple comparisons and the Wilcoxon–Duncan test. Origin 2024 (OriginLab, Northampton, MA, USA) was used for graphical visualization.

## 3. Results

### *3.1. Dust Retention Capacity per Unit Leaf Area*

3.1.1. Differences in Dust Retention Capacity per Unit Leaf Area Among Plant Functional Types

The dust retention capacity per unit leaf area of different plant species is presented in Figure 4. Significant interspecific differences were observed among tree species (Figure 4a) and shrubs (Figure 4b), whereas no significant differences were detected among herbaceous species (Figure 4c). The dust retention capacity per unit leaf area ranged from 1.53 to 22.28 g·m$^{-2}$. *Juniperus chinensis 'Kaizuca'* exhibited the highest dust retention capacity (22.28 g·m$^{-2}$), followed by *Juniperus chinensis L.* (18.63 g·m$^{-2}$) and *Rosa rugosa Thunb.* (13.70 g·m$^{-2}$). The subsequent ranking was *Platycladus orientalis (L.) Franco, Ulmus pumila 'Jinye', Prunus triloba Lindl., Rosa chinensis Jacq., Platanus acerifolia (Aiton) Willd., Catalpa speciosa (Warder ex Barney) Engelm., Ligustrum obtusifolium Siebold & Zucc., Malus spectabilis (Aiton) Borkh., Lolium perenne L., Fraxinus chinensis Roxb.*, and *Poa annua L.*, whereas *Amorpha fruticosa*

 doi:10.20944/preprints202602.0618.v1



*L.* exhibited the lowest dust retention capacity (1.53 g·m$^{-2}$). Among trees, *Juniperus chinensis 'Kaizuca'* showed the strongest dust retention capacity; among shrubs, *Juniperus chinensis L.* performed best; and among herbaceous species, *Lolium perenne L.* exhibited the highest dust retention capacity.

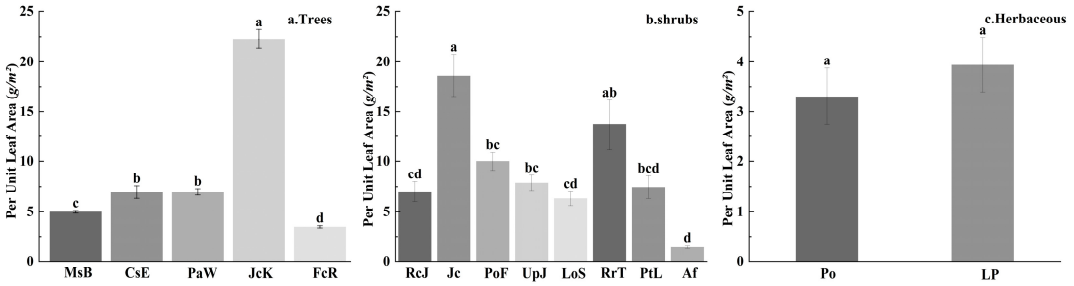


**Figure 4.** Dust retention per unit leaf area of different plant species. **MsB**: *Malus spectabilis (Aiton) Borkh.*; **CsE**: *Catalpa speciosa (Warder ex Barney) Engelm.*; **PaW**: *Platanus acerifolia (Aiton) Willd*; **JcK**: *Juniperus chinensis 'Kaizuca*'; **FcR**: *Fraxinus chinensis Roxb.*; **RcJ**: *Rosa chinensis Jacq.*; **Jc**: *Juniperus chinensis L.*; **PoF**: *Platycladus orientalis (L.) Franco*; **UpJ**: *Ulmus pumila 'Jinye'*; **LoS**: *Ligustrum obtusifolium Siebold & Zucc.*; **RrT**: *Rosa rugosa Thunb.*; **PtL**: *Prunus triloba Lindl.*; **Af**: *Amorpha fruticosa L.*; **Po**: *Poa annua L.*; **Lp**: *Lolium perenne L.*

3.1.2. Spatiotemporal Variation in Dust Retention Capacity per Unit Leaf Area

(1) Temporal variation. Significant temporal differences in dust retention capacity were observed among plant species from May to August (Figure 5). Cumulative data for the study period indicated that *Juniperus chinensis 'Kaizuca'* exhibited the highest dust retention capacity among tree species, while *Juniperus chinensis L.* showed the strongest capacity among shrubs. Among herbaceous species, *Lolium perenne L.* demonstrated higher dust retention than *Poa annua L.* For most species, except *Poa annua L.*, dust retention in June was significantly higher than in other months. Overall, dust retention followed the pattern: June > May > July > August. However, several species exhibited distinct seasonal patterns. For *Catalpa speciosa (Warder ex Barney) Engelm.*, dust retention followed the sequence June > July > May > August, likely because May corresponds to the leaf expansion stage, during which dust interception capacity is relatively low [24]. For *Juniperus chinensis 'Kaizuca'*, dust retention capacity followed the pattern May > July > June > August. As an evergreen species planted beneath tall *Platanus acerifolia (Aiton) Willd.* and *Malus spectabilis (Aiton) Borkh.*, its canopy openness is extremely low, which restricts airflow and reduces particulate deposition [25]. For *Poa annua L.*, dust retention capcity followed the sequence July > June > August > May, reflecting its slower early-season growth compared with *Lolium perenne L.* The retention efficiency follows the pattern: May > July > June > August. *Poa annua L.* exhibited slower growth in May and June compared to *Lolium perenne L* [26], reflecting its slower early-season growth compared with *Lolium perenne L.*

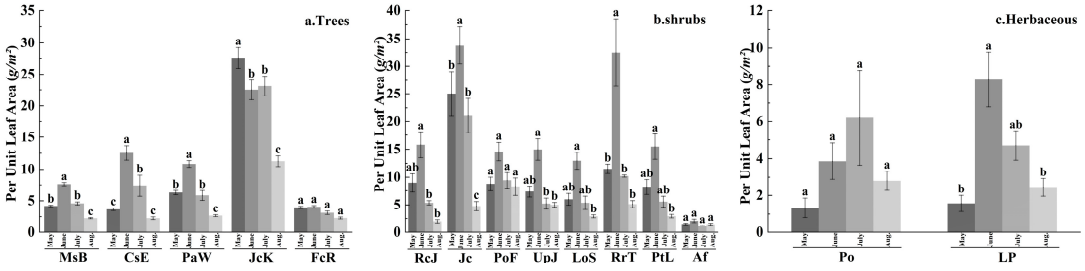


**Figure 5.** Dust retention capacity per unit leaf area in different months. **MsB**: *Malus spectabilis (Aiton) Borkh.*; **CsE**: *Catalpa speciosa (Warder ex Barney) Engelm.*; **PaW**: *Platanus acerifolia (Aiton) Willd*; **JcK**: *Juniperus chinensis 'Kaizuca*'; **FcR**: *Fraxinus chinensis Roxb.*; **RcJ**: *Rosa chinensis Jacq.*; **Jc**: *Juniperus chinensis L.*; **PoF**: *Platycladus orientalis (L.) Franco*; **UpJ**: *Ulmus pumila 'Jinye'*; **LoS**: *Ligustrum obtusifolium Siebold & Zucc.*; **RrT**: *Rosa rugosa Thunb.*; **PtL**: *Prunus triloba Lindl.*; **Af**: *Amorpha fruticosa L.*; **Po**: *Poa annua L.*; **Lp**: *Lolium perenne L.*

 doi:10.20944/preprints202602.0618.v1



(2) Spatial variation. No significant differences in dust retention were detected among horizontal directions; however, overall dust retention capacity was higher on the leeward side of traffic than on the windward side, and higher on the leeward roadside than on the windward roadside (Figure 6). In contrast, *Juniperus chinensis 'Kaizuca'*, *Rosa rugosa Thunb.*, and *Prunus triloba Lindl*. exhibited higher dust deposition on the windward side than on the leeward side. This pattern may be attributed to their location within the central strip of roadside green belts, where plants are exposed to airflow vortices that enhance particulate deposition on the windward side [27] .

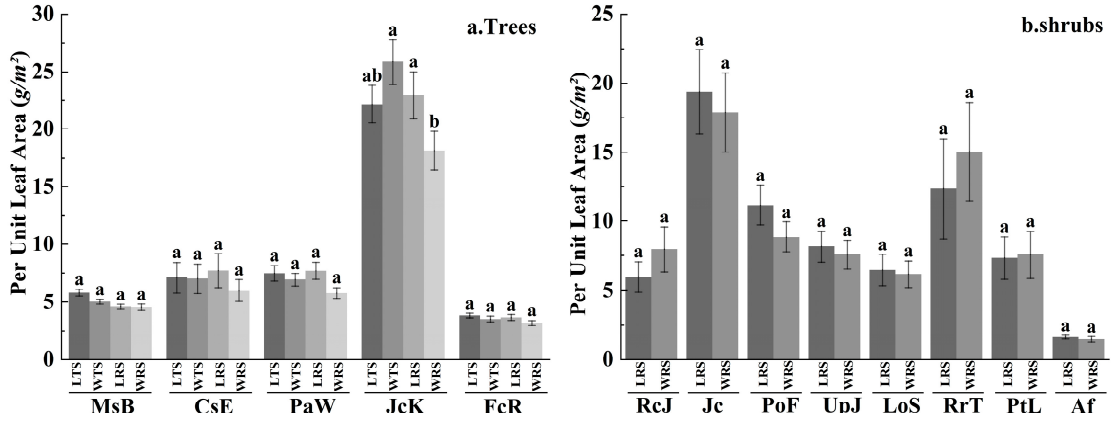


**Figure 6.** Dust retention capacity per unit leaf area of plants in different directions. **MsB**: *Malus spectabilis (Aiton) Borkh.*; **CsE**: *Catalpa speciosa (Warder ex Barney) Engelm.*; **PaW**: *Platanus acerifolia (Aiton) Willd*; **JcK**: *Juniperus chinensis 'Kaizuca'*; **FcR**: *Fraxinus chinensis Roxb.*; **RcJ**: *Rosa chinensis Jacq.*; **Jc**: *Juniperus chinensis L.*; **PoF**: *Platycladus orientalis (L.) Franco*; **UpJ**: *Ulmus pumila 'Jinye'*; **LoS**: *Ligustrum obtusifolium Siebold & Zucc.*; **RrT**: *Rosa rugosa Thunb.*; **PtL**: *Prunus triloba Lindl.*; **Af**: *Amorpha fruticosa L.*; **Po**: *Poa annua L.*; **Lp**: *Lolium perenne L.*; **LTS**: leeward side of traffic; **WTS**: Windward Traffic Side.; **LRS**: leeward roadside; **WRS**: Windward Roadside.

Vertical stratification significantly influenced dust retention in tree species. Except for *Juniperus chinensis 'Kaizuca'*, most tree species exhibited the pattern: middle canopy layer > lower layer > upper layer (Figure 7). In contrast, *Juniperus chinensis 'Kaizuca'* showed the pattern: lower layer > middle layer > upper layer, primarily due to its pyramidal crown architecture. In most tree species, oval or rounded crowns promote greater dust accumulation in the middle canopy layer, whereas the dense lower foliage of *Juniperus chinensis 'Kaizuca'* is directly exposed to vehicle-generated dust, resulting in higher particulate deposition in the lower layer [28]. Overall, dust retention capacity per unit leaf area differed significantly among plant functional types, following the pattern: shrubs > trees > herbaceous species (Figure 8) [29].

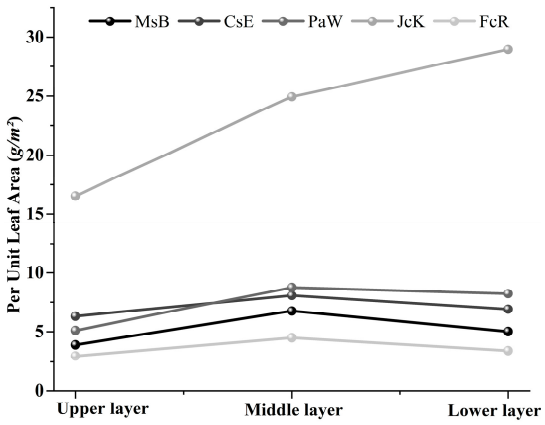


**Figure 7.** Changes in dust retention capacity per unit leaf area in the vertical direction of trees. **MsB**: *Malus spectabilis (Aiton) Borkh.*; **CsE**: *Catalpa speciosa (Warder ex Barney) Engelm.*; **PaW**: *Platanus acerifolia (Aiton) Willd*; **JcK**: *Juniperus chinensis 'Kaizuca'*; **FcR**: *Fraxinus chinensis Roxb.*

 doi:10.20944/preprints202602.0618.v1



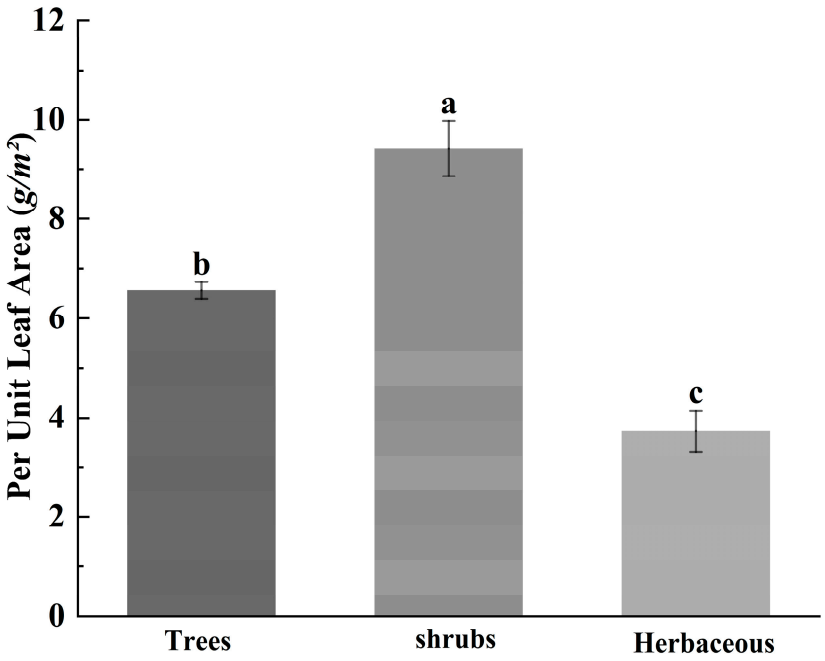


**Figure 8.** Dust retention capacity per unit leaf area for different plant types.

3.1.3. Relationships Between Leaf Surface Microstructure and Dust Retention Capacity

Analysis of leaf surface microstructural characteristics (Figure 9; Table 2) revealed pronounced interspecific differences in both macroscopic and microscopic features on the adaxial and abaxial leaf surfaces. Dust retention capacity was closely associated with leaf surface structure, reflecting the combined effects of multiple traits, including stomatal morphology and density, surface roughness, protrusions, wax layers, trichomes, and grooves.

**Table 2.** Leaf surface microstructural characteristics of roadside green space plant communities.

| Plant Name | Groove width | Stomatal parameters | | |
|---|---|---|---|---|
| | | Density | Aspect ratio | Protrusion |
| *Platanus acerifolia (Aiton) Willd* | 3.30±0.42 | 314.49±16.47 | 2.13±0.45 | protrusion |
| *Catalpa speciosa (Warder ex Barney) Engelm.* | 1.99±0.32 | 442.62±98.84 | 6.43±1.94 | level |
| *Malus spectabilis (Aiton) Borkh.* | 3.39±0.41 | 267.90±16.47 | 7.39±1.03 | level |
| *Fraxinus chinensis Roxb.* | 4.05±0.33 | 407.68±16.47 | 8.34±2.46 | protrusion |
| *Juniperus chinensis 'Kaizuca'* | 2.93±0.86 | 244.61±16.47 | 3.04±0.55 | level |
| *Ulmus pumila 'Jinye'* | 3.47±0.61 | 372.73±32.95 | 3.13±0.31 | protrusion |
| *Rosa rugosa Thunb.* | 3.97±0.58 | 209.66±32.95 | 6.74±2.46 | level |
| *Prunus triloba Lindl.* | 3.75±0.19 | 361.09±16.47 | 5.33±1.05 | level |
| *Ligustrum obtusifolium Siebold & Zucc.* | 4.01±0.45 | 361.09±16.47 | 3.30±0.82 | protrusion |
| *Rosa chinensis Jacq.* | 12.49±0.58 | 186.37±32.95 | 5.61±0.47 | level |
| *Amorpha fruticosa L.* | 5.77±0.55 | 128.13±16.47 | 24.34±10.35 | Indentation |
| *Platycladus orientalis (L.) Franco* | 3.27±0.67 | 221.31±16.47 | 2.51±0.30 | level |
| *Juniperus chinensis L.* | 4.57±0.32 | 337.79±16.47 | 5.86±1.66 | protrusion |
| *Lolium perenne L.* | 3.05±0.35 | 151.42±16.47 | 143.65±56.87 | level |
| *Poa annua L.* | 2.14±0.50 | 174.72±16.47 | 29.27±5.26 | Indentation |

Leaves of *Juniperus chinensis 'Kaizuca'* and *Juniperus chinensis L.* were characterized by abundant trichomes, coarse wax crystals, and well-developed grooves. Dense pubescence and deep epidermal grooves effectively trapped particulate matter within stomatal cavities and surface depressions, resulting in the highest dust retention per unit area. The abaxial epidermis of *Rosa rugosa Thunb.* exhibited numerous fine grooves and folds, forming irregular micro-concave structures that markedly increased surface roughness. A thin, adhesive wax layer with a finely granular texture

 doi:10.20944/preprints202602.0618.v1



further enhanced its dust retention capacity. *Platycladus orientalis (L.) Franco* displayed prominently raised stomata and a thick wax layer, which facilitated the adsorption of particulate matter along stomatal margins and within surface grooves, leading to relatively high dust retention. *Ulmus pumila 'Jinye'*, *Prunus triloba Lindl.*, and *Rosa chinensis Jacq.* possessed moderate levels of pubescence and surface grooves, as well as intermediate stomatal densities. In contrast, *Ligustrum obtusifolium Siebold & Zucc.*, *Malus spectabilis (Aiton) Borkh.*, *Lolium perenne L.*, *Fraxinus chinensis Roxb.*, *Poa annua L.*, and *Amorpha fruticosa L.* exhibited relatively smooth leaf surfaces with thin wax layers and sparse microstructural features. Their surfaces were more susceptible to particle erosion, resulting in the lowest dust retention capacity per unit leaf area.

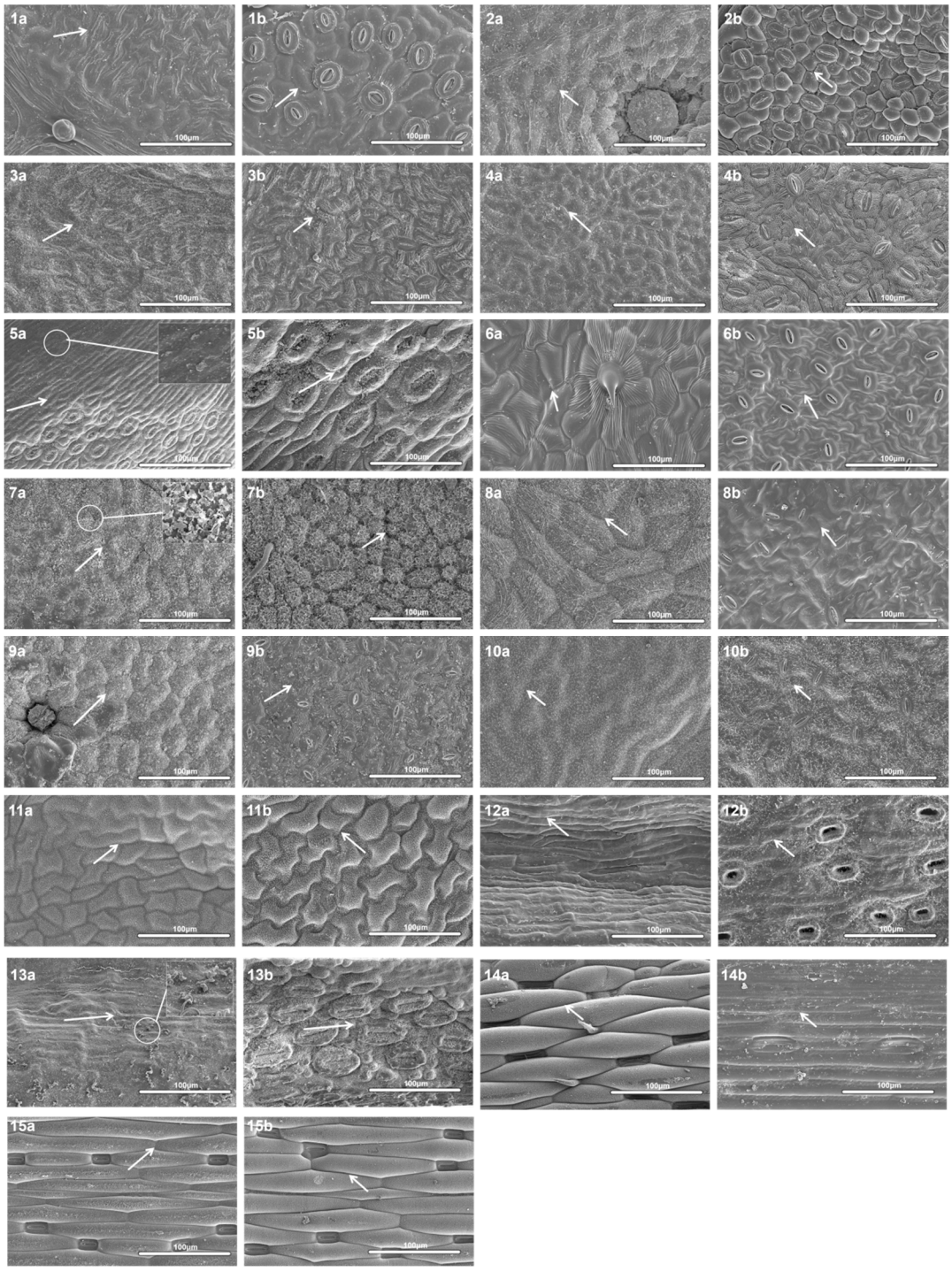


**Figure 9.** Leaf surface microstructures of different plant species. Schemes follow the same formatting. **1.** *Platanus acerifolia (Aiton) Willd*; **2.** *Catalpa speciosa (Warder ex Barney) Engelm.*; **3.** *Malus spectabilis (Aiton) Borkh.*; **4.** ***Fraxinus chinensis Roxb.***; **5.** ***Juniperus chinensis 'Kaizuca'***; **6.** ***Ulmus pumila 'Jinye'***; **7.** *Rosa rugosa Thunb.*; **8.** *Prunus triloba*

 doi:10.20944/preprints202602.0618.v1



*Lindl.*; **9.** *Ligustrum obtusifolium Siebold & Zucc.*; **10.** *Rosa chinensis Jacq.*; **11.** *Amorpha fruticosa L.*; **12.** *Platycladus orientalis (L.) Franco*; **13.** *Juniperus chinensis L.*; **14.** *Lolium perenne L.*; **15.** *Poa annua L.*; **a represents the upper surface of the leaf; b represents the lower surface of the leaf.**

### *3.2. Dust Retention Capacity of Individual Plants*

Significant differences in dust retention capacity were observed among individual plants ($P < 0.05$), with values ranging from 0.008 to 2.91 kg·plant$^{-1}$ (Figure 10). Among tree species, *Platanus acerifolia (Aiton) Willd*. exhibited the highest dust retention capacity (2.909 kg·plant$^{-1}$), followed by *Fraxinus chinensis Roxb*. (1.487 kg·plant$^{-1}$), *Juniperus chinensis 'Kaizuca'* (1.467 kg·plant$^{-1}$), and *Malus spectabilis (Aiton) Borkh*. (1.138 kg·plant$^{-1}$). *Catalpa speciosa (Warder ex Barney) Engelm*. showed the lowest capacity (0.513 kg·plant$^{-1}$). Among shrubs, *Rosa rugosa Thunb*. exhibited the highest dust retention capacity (0.161 kg·plant$^{-1}$), followed by *Prunus triloba Lindl*., *Juniperus chinensis L*., *Platycladus orientalis (L.) Franco*, *Ulmus pumila 'Jinye'*, *Rosa chinensis Jacq*., and *Ligustrum obtusifolium Siebold & Zucc*. *Amorpha fruticosa L*. exhibited the lowest capacity (0.018 kg·plant$^{-1}$). Among herbaceous species, *Lolium perenne L*. showed relatively high dust retention (0.009 kg·plant$^{-1}$), whereas *Poa annua L*. exhibited the lowest capacity (0.008 kg·plant$^{-1}$).

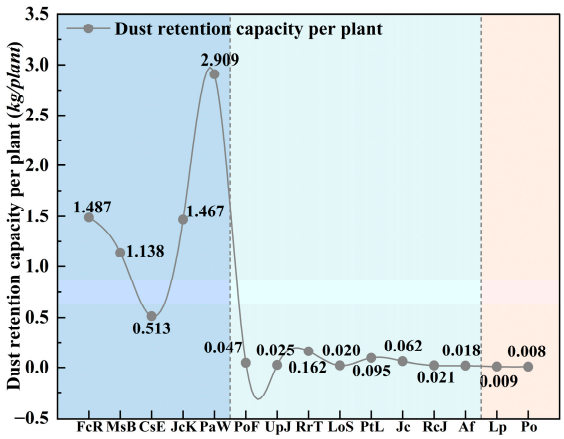


**Figure 10.** Dust retention capacity of individual plants of different species. **PaW**: *Platanus acerifolia (Aiton) Willd*; **CsE**: *Catalpa speciosa (Warder ex Barney) Engelm*.; **MsB**: *Malus spectabilis (Aiton) Borkh*.; **FcR**: *Fraxinus chinensis Roxb*.; **JcK**: *Juniperus chinensis 'Kaizuca*'; **UpJ**: *Ulmus pumila 'Jinye'*; **RrT**: *Rosa rugosa Thunb*.; **PtL**: *Prunus triloba Lindl*.; **LoS**: *Ligustrum obtusifolium Siebold & Zucc*.; **Rc**: *Rosa chinensis Jacq*.; **Af**: *Amorpha fruticosa L*.; **PoF**: *Platycladus orientalis (L.) Franco*; **Jc**: *Juniperus chinensis L*.; **Lp**: *Lolium perenne L*.; **Po**: *Poa annua L*.

### *3.3. Dust Retention Capacity of Plant Communities*

The dust retention capacities of different plant communities are presented in Figure 11. Community-level dust retention ranged from 0.467 to 0.955 kg·m$^{-2}$. Community 4# exhibited the highest dust retention capacity (0.955 kg·m$^{-2}$), followed by Communities 1#, 8#, 7#, 2#, and 6#, with values of 0.795, 0.773, 0.624, 0.623, and 0.604 kg·m$^{-2}$, respectively. Communities 5# and 3# exhibited the lowest capacities, with values of 0.513 and 0.467 kg·m$^{-2}$, respectively.

Comparative analysis of vegetation configuration patterns revealed that the tree–shrub–herbaceous and tree–herbaceous models exhibited higher dust retention capacities (0.704 and 0.709 kg·m$^{-2}$, respectively), whereas the tree–shrub model showed lower dust retention (0.558 kg·m$^{-2}$). Significant differences in dust retention were observed among the three configuration patterns. In the tree–herbaceous and tree–shrub–herbaceous models, shrubs and herbaceous plants occupy a larger proportion of the plot area and are distributed closer to the ground, enabling them to effectively intercept particulate matter generated by road traffic. Meanwhile, tree canopies capture a substantial proportion of airborne particles within the vertical airflow, thereby enhancing overall dust retention at the community level.

 doi:10.20944/preprints202602.0618.v1



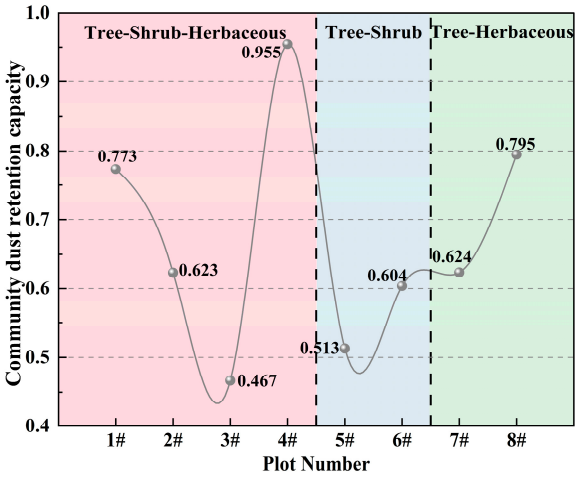


**Figure 11.** Dust retention capacity of different plant communities.

## 4. Discussion

Significant interspecific differences in dust retention per unit leaf area were observed, indicating that plant dust retention capacity arises from the synergistic effects of multiple morphological and structural traits. Although numerous studies have explored interspecific variation in dust retention, most have been conducted under humid climatic conditions. In contrast, this study focuses on the ecologically fragile region of southern Xinjiang, where dust storms occur frequently, and systematically investigates dust retention characteristics at both individual plant and community levels.

### *4.1. Dust Retention Capacity of Individual Plants*

Path analysis is an effective method for elucidating the relationships between multiple independent variables and a dependent variable, typically implemented through stepwise regression analysis. In this process, independent variables are sequentially introduced into the regression model according to their statistical significance and relative contribution to the dependent variable, while variables with insignificant effects are eliminated. Thus, path analysis enables the identification and ranking of key factors influencing the dependent variable [30]. In this study, dust retention per unit leaf area was treated as the dependent variable, and leaf surface structural characteristics were used as independent variables. Path analysis (via stepwise regression) was applied to explore the mechanisms governing dust retention in different plant species. The results are presented in Table 3.

**Table 3.** Regression coefficient results.

| Model | Unstandardized coefficient | | Standardized Coefficient | t | Significance |
|---|---|---|---|---|---|
| | B | Standard Error | Regression coefficient | | |
| (Constant) | 0.184 | 0.131 | | 1.399 | 0.174 |
| Leaf aspect ratio | 0.027 | 0.004 | 0.583 | 6.009 | 0 |
| Aspect ratio of stomatals | -0.005 | 0.001 | -0.448 | -4.329 | 0 |
| Stomatals protrusion | 0.083 | 0.036 | 0.235 | 2.318 | 0.029 |
| Groove width | 0.022 | 0.009 | 0.266 | 2.492 | 0.02 |
| Roughness | 0.199 | 0.051 | 0.421 | 3.931 | 0.001 |

Note: Significance ($P < 0.05$).

 doi:10.20944/preprints202602.0618.v1



Previous studies have reported that dust retention capacity can differ by more than two- to threefold among tree species [31]. Here, the leaf surface structures of 15 plant species were examined using macroscopic observation and electron microscopy to clarify how leaf surface traits influence dust retention (Table 3). The results indicate that leaf aspect ratio and surface roughness are key factors promoting dust deposition [32,33]. A larger leaf aspect ratio may be associated with greater effective surface area and specific morphological features that facilitate stable particle adhesion. This finding is consistent with previous reports by Liu [34] and Wang [35]. *Juniperus chinensis 'Kaizuca'* and *Juniperus chinensis L.* exhibit narrow leaves with distinctive cuticular textures or dense pubescence. Their leaf surfaces are characterized by abundant trichomes, coarse wax crystals, and well-developed grooves. These features satisfy two critical conditions for dust retention—airflow modulation and increased attachment sites—thereby conferring high dust retention capacity. In contrast, *Platanus acerifolia (Aiton) Willd.*, *Malus spectabilis (Aiton) Borkh.*, and *Fraxinus chinensis Roxb.* possess broader leaves with relatively smoother surfaces. Airflow over such surfaces tends to be laminar, reducing particle collision frequency. Moreover, adhered particles are more easily removed by precipitation or strong winds, resulting in lower dust retention per unit leaf area [36]. These findings are consistent with previous studies by Myeong [37], Bridhikitti [38], Sheng [40], and Gao [40].

Path analysis further revealed that stomatal aspect ratio exerts a significant negative direct effect on dust retention capacity: the more elongated the stomata, the lower the dust retention capacity. However, when interactions among traits were considered, stomatal aspect ratio exhibited a positive indirect effect mediated by stomatal protrusion. This suggests that elongated stomata alone are unfavorable for dust retention, but pronounced protruding structures can partially offset their negative influence. Groove width showed a significant positive direct effect on dust retention capacity, whereas surface roughness produced a negative indirect effect (−0.118). This indicates that excessively wide grooves may reduce overall surface roughness and, consequently, the number of effective particle attachment sites. Such trade-offs help explain inconsistencies reported in previous microstructural–functional studies. For example, Pu et al. emphasized the positive role of grooves [41], likely focusing on their direct reservoir function, whereas Huang et al. highlighted their negative effect [42]. Studies that identify roughness as the dominant factor emphasize surface adhesion capacity [43]. Correlation analysis confirms that groove morphology and roughness interact synergistically, suggesting that optimal dust retention depends on the coordinated configuration of these traits. Future research should quantitatively characterize the spatial geometric relationship between groove morphology and surface roughness at finer scales to further verify this trade-off mechanism.

**Table 4.** Analysis of dust retention capacity per unit leaf area and leaf surface structural stomatal diameter.

| factor | Direct Passage Coefficient | Indirect Passage Coefficient | | | | |
|---|---|---|---|---|---|---|
| | | Leaf aspect ratio | Aspect ratio of stomatals | Stomatals protrusion | Groove width | Roughness |
| Leaf aspect ratio | 0.583 | | 0.104 | -0.015 | -0.087 | 0.099 |
| Aspect ratio of stomatals | -0.448 | -0.080 | | 0.151 | 0.084 | -0.049 |
| Stomatals protrusion | 0.235 | -0.006 | -0.079 | | -0.001 | 0.028 |
| Groove width | 0.266 | -0.040 | -0.050 | -0.001 | | -0.118 |
| Roughness | 0.421 | 0.071 | 0.046 | 0.051 | -0.187 | |

Growth characteristics of tree species—including tree height, crown height, crown width, and branch-free height—significantly influence total leaf area per tree [44], thereby affecting dust

 doi:10.20944/preprints202602.0618.v1



retention capacity at the individual level. This study demonstrates that dust deposition per plant is jointly determined by total leaf area and leaf area index (Figure 12), consistent with the findings of Tao [45] and Li [46]. Even when dust retention capacity per unit area is not maximal, plants with large size and extensive leaf area can exhibit high overall dust retention capacity [47]. Broadleaf species generally exhibit greater tree height, crown spread, and branch-free height than conifers, resulting in significantly higher dust retention capacity per individual tree [48]. Although *Juniperus chinensis 'Kaizuca'* shows high dust retention capacity per unit leaf area, its relatively small crown spread and total leaf area limit its overall dust retention capacity. Conversely, *Platanus acerifolia (Aiton) Willd*. exhibits moderate dust retention capacity per unit area but achieves high per-tree retention due to its broad canopy and abundant foliage. Therefore, when evaluating dust retention performance, tree species with large total leaf area should be prioritized.

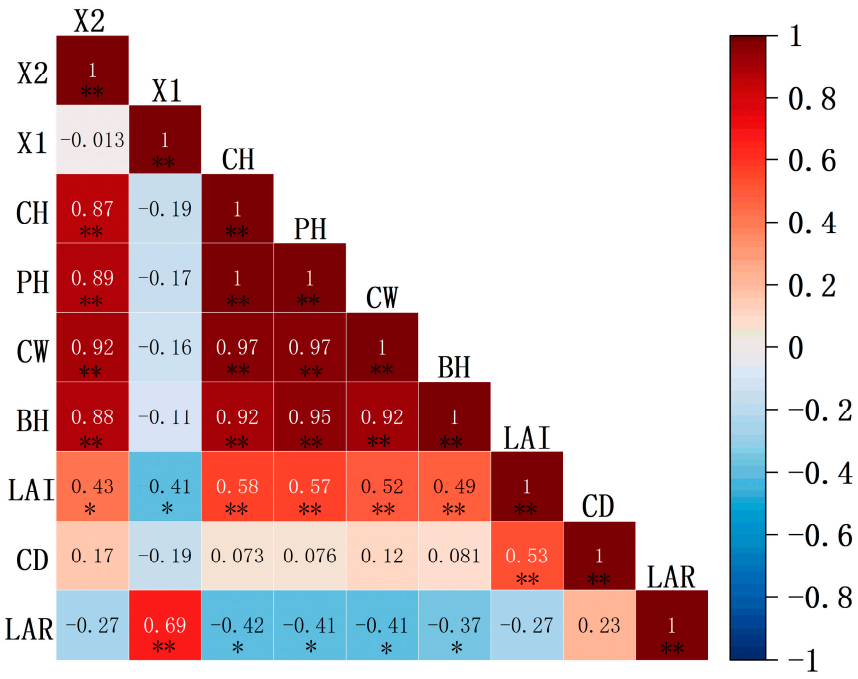


**Figure 12.** Correlation analysis of factors affecting dust retention capacity per plant.**X1**: Dust retention per unit leaf area; **X2**: Dust retention per individual tree; **CH**: Crown height; **PH**: Plant height; **CW**: Crown width; **BH**: Branch height; **LAI**: Leaf area index; **CD**: Canopy density; **LAR**: Leaf aspect ratio.

### *4.2. Particulate Matter Retention Capacity of Plant Communities*

The results indicate that plant communities with a multi-layered vertical structure composed of trees, shrubs, and herbaceous exhibit significantly higher dust retention capacity than single-layer green space configurations. Increased vertical stratification enhances dust retention effectiveness, consistent with previous studies [49]. The spatial structure and configuration of plant communities are critical determinants of atmospheric particulate matter deposition [50]. In tree–herb communities, dense foliage in both the tree and herbaceous layers is less susceptible to airflow disturbance, resulting in superior dust retention capacity. In shrub-dominated communities, shrubs are more vulnerable to wind and anthropogenic disturbance, leading to lower dust retention compared with tree–herb communities [51].

Significant differences in dust retention capacity were observed among plant communities, likely due to the combined effects of species composition and spatial configuration. Dust retention capacity at the individual-tree level is a key determinant of community-level performance. Using the entropy-weighted method to comprehensively evaluate plant communities based on species diversity, configuration patterns, dust retention capacity, dust retention capacity per unit leaf area, dust retention capacity per individual plant, community cooling rate, and humidification rate (Table 5),

 doi:10.20944/preprints202602.0618.v1



communities dominated by *Platanus acerifolia (Aiton) Willd*. (No. 4# and No. 6#) achieved significantly higher comprehensive scores than other communities. This result is consistent with previous findings by Sun [52] and Zhang [53]. Notably, in communities dominated by *Malus spectabilis (Aiton) Borkh*., plots 1# and 5# exhibited higher species richness than plots 2# and 7#, highlighting the influence of species richness and structural diversity on dust retention capacity, in agreement with Zhang [54] and Liu [55]. Tree–shrub–herb communities exhibited stronger dust retention than tree–herb communities. Within the study plots, Plot 2 outperformed Plot 7, and Plot 3 outperformed Plot 8, likely due to differences in wind speed and direction, which may cause particulate matter deposited on leaves to migrate into the shrub layer, combined with secondary dust resuspension from traffic.

**Table 5.** Weighted evaluation indicators for selecting comprehensive dust retention capacity models in typical roadside green space communities using the entropy method.

| Indicator | Standardization Matrix | | | | | | | | Entropy values and weights | | |
|---|---|---|---|---|---|---|---|---|---|---|---|
| Community | 1# | 2# | 3# | 4# | 5# | 6# | 7# | 8# | ej | gj | wj |
| X1 | 0.6442 | 0.5590 | 0.0001 | 0.4038 | 0.9152 | 1.0001 | 0.2577 | 0.2263 | 0.8765 | 0.1235 | 0.0884 |
| X2 | 0.0001 | 0.1341 | 0.1866 | 0.4322 | 0.0561 | 1.0001 | 0.2247 | 0.3453 | 0.7827 | 0.2173 | 0.1556 |
| CDRC | 0.3509 | 0.0702 | 0.0001 | 0.2289 | 0.4130 | 1.0001 | 0.1117 | 0.2181 | 0.7882 | 0.2118 | 0.1517 |
| PS | 0.6668 | 0.0001 | 0.0001 | 1.0001 | 0.3334 | 0.3334 | 0.0001 | 0.0001 | 0.6149 | 0.3851 | 0.2758 |
| CM | 1.0001 | 1.0001 | 1.0001 | 1.0001 | 0.5001 | 0.5001 | 0.0001 | 0.0001 | 0.8408 | 0.1592 | 0.1140 |
| T | 1.0001 | 0.3000 | 0.1544 | 0.6576 | 0.5677 | 0.5092 | 0.4066 | 0.0001 | 0.8772 | 0.1228 | 0.0880 |
| RH | 1.0001 | 0.3519 | 0.1977 | 0.3432 | 0.4445 | 0.0372 | 0.5397 | 0.0001 | 0.8232 | 0.1768 | 0.1266 |
| Si | 0.6225 | 0.2658 | 0.1816 | 0.6287 | 0.4073 | 0.5941 | 0.1787 | 0.1068 | | | |

**X1**: Dust retention per unit leaf are; **X2**: Dust retention capacity per plant; **CDRC**: Community dust retention capacity; **PS**: Plant species; **CM**: Configura-tion Mode; **T**: Community cooling rate; **RH**: Community Humidification Rate; **Si**: Comprehensive Score; **ej**: Information entropy; **gj**: Coefficient of Variation; **wj**: Weight.

Overall, this study identifies dominant species and clarifies particulate matter retention mechanisms in roadside green spaces at both individual and community scales. Community-level particulate matter retention depends not only on dust retention capacity per unit leaf area and per individual plant, but also on tree growth characteristics, community configuration patterns, species richness, and structural diversity. For urban roadside green spaces in arid regions of southern Xinjiang, it is recommended to adopt a spatial structure characterized by "vertical stratification and a mix of evergreen and deciduous species." The canopy should be anchored by high dust-retention species such as *Platanus acerifolia (Aiton) Willd.*, complemented by evergreen species such as *Juniperus chinensis 'Kaizuca'* to maintain dust retention during winter. Shrubs should include *Juniperus chinensis L.* and *Rosa rugosa Thunb*., with *Lolium perenne L.* as the herbaceous layer, forming a multi-layered tree–shrub–herb structure. Monoculture planting patterns should be avoided. Enhancing shrub layers and species diversity can maximize dust retention benefits while achieving optimal integration of aesthetic, ecological, and functional values.

This study employed the entropy-weighted method as an objective approach to evaluate community-level particulate matter retention. To improve the perceptual relevance of evaluation indicators, future studies should incorporate subjective assessment metrics, such as public satisfaction surveys and perceived health impacts. Such integration would yield results more closely aligned with societal needs.

Furthermore, plant dust retention is a dynamic process influenced by environmental variability. Future research should integrate dynamic monitoring of leaf surface microstructure, environmental factors, and dust retention mechanisms. Establishing a long-term monitoring platform is

 doi:10.20944/preprints202602.0618.v1



recommended to track temporal changes in leaf microstructure (e.g., via scanning electron microscopy), real-time environmental parameters (wind speed, humidity, particulate composition and concentration, precipitation intensity), and dynamic variations in dust deposition and deposition rates.

## 5. Conclusions

Roadside green spaces function as critical ecological barriers in urban environments, with plant communities playing a key role in improving regional air quality. This study investigated typical roadside plant communities in southern Xinjiang, a region characterized by extreme aridity and frequent dust storms. By measuring dust retention at individual and community levels and analyzing leaf surface microstructure, we evaluated the comprehensive dust retention performance of different community configuration patterns. The main conclusions are as follows:

(1) Spatiotemporal variation in dust retention capacity per unit leaf area: *Juniperus chinensis 'Kaizuca'* exhibited the strongest dust retention capacity, followed by *Juniperus chinensis L.* and *Rosa rugosa Thunb*. Dust retention followed the seasonal pattern June > May > July > August. Horizontally, both trees and shrubs showed higher dust retention on the leeward side of roads than on the windward side. Vertically, dust retention in trees followed the pattern middle layer > lower layer > upper layer. Leaf dust retention is governed by the combined effects of multiple factors, including leaf aspect ratio, stomatal aspect ratio, stomatal protrusion, stomatal density, wax layer characteristics, and surface roughness. Leaf aspect ratio exerted a significant positive direct effect, whereas stomatal aspect ratio showed a significant negative direct effect on dust retention.

(2) Dust retention capacity per plant: Among trees, *Platanus acerifolia (Aiton) Willd*. exhibited the highest dust retention capacity, followed by *Fraxinus chinensis Roxb*., *Juniperus chinensis 'Kaizuca'*, and *Malus spectabilis (Aiton) Borkh*. Among shrubs, *Rosa rugosa Thunb*. showed relatively high dust retention, followed by *Prunus triloba Lindl*., *Juniperus chinensis L.*, *Platycladus orientalis (L.) Franco*, *Ulmus pumila 'Jinye'*, *Rosa chinensis Jacq*., and *Ligustrum obtusifolium Siebold & Zucc*., whereas *Amorpha fruticosa L.* exhibited the lowest capacity. Among herbaceous species, *Lolium perenne L.* demonstrated relatively strong dust retention, while *Poa annua L.* showed the weakest performance. Per-plant dust retention is strongly influenced by total leaf area and leaf area index, leading to higher overall retention than that indicated by unit-area measurements alone.

(3) Dust retention capacity of plant communities and configuration patterns: Tree–shrub–herb and tree–herb configuration patterns exhibited stronger dust retention than tree–shrub patterns. Community spatial structure and configuration are key determinants of atmospheric particulate matter deposition. Multi-layered communities centered on *Platanus acerifolia (Aiton) Willd*. achieved optimal synergy among dust retention, landscape aesthetics, and ecological functions. These findings provide empirical evidence and optimization strategies for plant selection and sustainable landscape design in roadside green spaces in southern Xinjiang and other arid regions.

**Author Contributions:** Conceptualization, F. W. and J. Y.; methodology, R. L.; software, F. C.; validation, F. W; formal analysis, F. W.; investigation, F. C.; resources, F. W.; data curation, F. W.; writing—original draft preparation, F. W.; writing—review and editing, J. Y.; visualization, R. L.; supervision, J. Y.; project administration, R. L.; funding acquisition, R. L. All authors have read and agreed to the published version of the manuscript.

**Funding:** The research was supported by the Key Research and Development Program of the Xinjiang Uygur Autonomous Region (No. 2024B04031-2).

**Data Availability Statement:** The data that support the findings of this study are available from the corresponding author upon reasonable request.

**Conflicts of Interest:** The authors declare no conflicts of interest.

## References

 doi:10.20944/preprints202602.0618.v1




1. Lelieveld, J.; Evans, J.S.; Fnais, M.; Giannadaki, D.; Pozzer, A. The Contribution of Outdoor Air Pollution Sources to Premature Mortality on a Global Scale. *Nature* **2015**, *525*, 367-371, doi:10.1038/nature15371.
2. Schraufnagel, D.E.; Balmes, J.R.; Cowl, C.T.; De Matteis, S.; Jung, S.-H.; Mortimer, K.; Perez-Padilla, R.; Rice, M.B.; Riojas-Rodriguez, H.; Sood, A.; et al. Air Pollution and Noncommunicable Diseases. *Chest* **2019**, *155*, 409-416, doi:10.1016/j.chest.2018.10.042.
3. Wen, Z.; Ma, X.; Xu, W.; Si, R.; Liu, L.; Ma, M.; Zhao, Y.; Tang, A.; Zhang, Y.; Wang, K.; et al. Combined Short-Term and Long-Term Emission Controls Improve Air Quality Sustainably in China. *Nature Communications* **2024**, *15*, doi:10.1038/s41467-024-49539-9.
4. Meo, S.A.; Salih, M.A.; Alkhalifah, J.M.; Alsomali, A.H.; Almushawah, A.A. Environmental Pollutants Particulate Matter (PM2.5, PM10), Carbon Monoxide (CO), Nitrogen Dioxide (NO2), Sulfur Dioxide (SO2), and Ozone (O3) Impact on Lung Functions. *Journal of King Saud University - Science* **2024**, *36*, 103280, doi:10.1016/j.jksus.2024.103280.
5. Hussein, T., Li, X., Al-Dulaimi, Q., Daour, S., Atashi, N., Viana, M., ... & Petäjä, T. (2020). Particulate matter concentrations in a Middle Eastern City—An insight to sand and dust storm episodes. *Aerosol and Air Quality Research*, 20(12), 2780-2792., https://doi.org/10.4209/aaqr.2020.05.0195.
6. Blessing Aibhamen Edeigba; Ugochukwu Kanayo Ashinze; Aniekan Akpan Umoh; Preye Winston Biu; Andrew Ifesinachi Daraojimba Urban green spaces and their impact on environmental health: A Global Review. *World Journal of Advanced Research and Reviews* **2024**, *21*, 917-927, doi:10.30574/wjarr.2024.21.2.0518.
7. Sillars-Powell, L.; Tallis, M.J.; Fowler, M. Road Verge Vegetation and the Capture of Particulate Matter Air Pollution. *Environments* **2020**, *7*, 93, doi:10.3390/environments7100093.
8. Wang; A.; Guo; Y.; Fang; Y.; Lu; K. Research on the Horizontal Reduction Effect of Urban Roadside Green Belt on Atmospheric Particulate Matter in a Semi-Arid Area. *Urban Forestry & Urban Greening* **2022** ,doi:**10.1016/j.ufug.2021.127449**.
9. Liu, Z.; Rieder, H.E.; Schmidt, C.; Mayer, M.; Guo, Y.; Winiwarter, W.; Zhang, L. Optimal Reactive Nitrogen Control Pathways Identified for Cost-Effective PM2.5 Mitigation in Europe. *Nature Communications* **2023**, *14*, doi:10.1038/s41467-023-39900-9.
10. Baidourela, A. , & Zhayimu, K. (2015). Patterns of dust retention by urban trees in oasis cities. *Nature Environment and Pollution Technology*, 14(1), 53-57, 53-57. https://neptjournal.com/upload-images/NL-51-10-(8)D-142.pdf
11. Tan; Yan., X.; Liu; Lu.; Wu; Ya., D. Relationship between Leaf Dust Retention Capacity and Leaf Microstructure of Six Common Tree Species for Campus Greening. *International journal of phytoremediation* **2022**, *24*, 1213-1221, https://doi.org/10.1080/15226514.2021.2024135.
12. Park, S.H.; Gong, S.L.; Gong, W.; Makar, P.A.; Moran, M.D.; Zhang, J.; Stroud, C.A. Relative Impact of Windblown Dust versus Anthropogenic Fugitive Dust in $PM_{2.5}$ on Air Quality in North America. *Journal of Geophysical Research: Atmospheres* **2010**, *115*, doi:10.1029/2009JD013144.
13. Liu; J; Ding; JL; Rexiding; M; Li; XH; Zhang; JY; et al. Characteristics of Dust Aerosols and Identification of Dust Sources in Xinjiang, China. *ATMOSPHERIC ENVIRONMENT* **2021**, *262*, 118651, doi:10.1016/j.atmosenv.2021.118651.
14. Jiang, B., Sun, C., Mu, S., Zhao, Z., Chen, Y., Lin, Y., Qiu, L., & Gao, T. (2022). Differences in Airborne Particulate Matter Concentration in Urban Green Spaces with Different Spatial Structures in Xi'an, China. *Forests*, 13(1), 14. https://doi.org/10.3390/f13010014
15. Singh, R.; Chavan, S.B.; Tomar, A.; Singh, H.; Chauhan, V.; Paul, N.; Singh, A.K. Species Variation in Air Pollution Tolerance, Performance, and Dust Retention of Urban Roadside Trees: Implications for Urban Greening and Green Corridor Planning. *Air Quality, Atmosphere & Health* **2025**, *18*, 3311-3327, doi:10.1007/s11869-025-01841-1.
16. Sheng, Q., Guo, Y., Lu, J., Song, S., Li, W., Yang, R., & Zhu, Z. (2024). A Study on the Dust Retention Effect of the Vegetation Community in Typical Urban Road Green Spaces—In the Case of Ying Tian Street in Nanjing City. *Sustainability*, 16(7), 2656, https://doi.org/10.3390/su16072656.
17. Zhang, X.-X.; Yang, X.-H.; Yang, F.; Lei, J.-Q.; Ali, M.; Li, S.-Y.; Liu, L.-Y.; Xue, Y.-B.; Wang, Z.-F.; Tian, W.-J.; et al. Windblown Dust in the Tarim Basin, Northwest China. *Scientific Reports* **2025**, *15*, doi:10.1038/s41598-025-95974-z.

18. Dang, N., Zhang, H., Li, H., Salam, M. M. A., & Chen, G. (2022). Comprehensive Evaluation of Dust Retention and Metal Accumulation by the Leaves of Roadside Plants in Hangzhou among Seasons. *Forests,* 13(8), 1290. https://doi.org/10.3390/f13081290
19. Baesso Moura, B., Zammarchi, F., Hoshika, Y., Martinelli, F., Paoletti, E., & Ferrini, F. (2024). Comparing Different Methodologies to Quantify Particulate Matter Accumulation on Plant Leaves. *Urban Science,* 8(3), 125. https://doi.org/10.3390/urbansci8030125
20. Kwak, M. J., Lee, J. K., Park, S., Kim, H., Lim, Y. J., Lee, K.-A., Son, J.-a., Oh, C.-Y., Kim, I., & Woo, S. Y. (2020). Surface-Based Analysis of Leaf Microstructures for Adsorbing and Retaining Capability of Airborne Particulate Matter in Ten Woody Species. *Forests,* 11(9), 946. https://doi.org/10.3390/f11090946.
21. Yan; Qian; Xu; Lishuai; Duan; Yonghong; Pan; Lichao; Wu; Zhangwei; et al. Influence of Leaf Morphological Characteristics on the Dynamic Changes of Particulate Matter Retention and Grain Size Distributions. *Environmental Technology* **2024**, *45*, 108-119, https://doi.org/10.1080/09593330.2022.2100281.
22. Yin, Z., Zhang, Y., & Ma, K. (2022). Evaluation of PM2.5 Retention Capacity and Structural Optimization of Urban Park Green Spaces in Beijing. Forests, 13(3), 415. https://doi.org/10.3390/f13030415
23. Zhou, Y.; Zhang, Z.; Lei, H.; Chen, X.; Yu, W.; Xu, Y.; Jiang, W. Evaluation and Obstacle Factors of the Green Development Level of Mature Resource-Based Cities Based on Entropy Weight TOPSIS Model: A Case Study of Daqing City in China. *Polish Journal of Environmental Studies* **2025**, *34*, 2979-2989, doi:10.15244/pjoes/188048.
24. Wang, H., Xing, Y., Yang, J., Xie, B., Shi, H., & Wang, Y. (2022). The Nature and Size Fractions of Particulate Matter Deposited on Leaves of Four Tree Species in Beijing, China. *Forests,* 13(2), 316. https://doi.org/10.3390/f13020316
25. He, D.; Yuan, J.; Lin, R.; Xie, D.; Wang, Y.; Kim, G.; Lei, Y.; Li, Y. Impact of Atmospheric Particulate Matter Retention on Physiological Characters of Five Plant Species under Different Pollution Levels in Zhengzhou. *PeerJ* **2024**, *12*, e18119, doi:10.7717/peerj.18119.
26. Wang, J., Li, H., Gong, D., Liu, X., Liu, B., & Guo, X. (2025). Physiological Responses and the Dust Retention Ability of Different Turfgrass Mixture Ratios Under Continuous Drought. *Plants*, 14(11), 1667, https://doi.org/10.3390/plants14111667.
27. Kim, Y. U., Lee, S. B., Kim, C. H., Lee, S., & Kwak, K. H. (2025). Aerodynamic and Dry Deposition Effects of Roadside Trees on NOx Concentration Changes on Roadways and Sidewalks. *Atmosphere*, 16(3), 344, https://doi.org/10.3390/atmos16030344.
28. Qin, H.; Hong, B.; Huang, B.; Cui, X.; Zhang, T. How Dynamic Growth of Avenue Trees Affects Particulate Matter Dispersion: CFD Simulations in Street Canyons. *Sustainable Cities and Society* **2020**, *61*, 102331, doi:10.1016/j.scs.2020.102331.
29. Mori, J., Fini, A., Galimberti, M., Ginepro, M., Burchi, G., Massa, D., & Ferrini, F. (2018). Air pollution deposition on a roadside vegetation barrier in a Mediterranean environment: Combined effect of evergreen shrub species and planting density. *Science of the total environment*, 643, 725-737, doi:10.1016/j.scitotenv.2018.06.217.
30. Kiani, B.; Soltanabadi, F.; Azimzadeh, H.; Moradi, G.H.; Esmaeilpour, M. Estimating and Simulating Dust Absorption Ability by Eldar Pine, Oriental Arbor-Vitae, River Red Gum and European Olive. *International Journal of Environmental Science and Technology* **2024**, *21*, 9977-9986, doi:10.1007/s13762-024-05773-8.
31. Xu; Lishuai; Yan; Qian; He; Peng; Zhen; Zhilei; Jing; Yaodong; et al. Combined Effects of Different Leaf Traits on Foliage Dust-Retention Capacity and Stability. *Air Quality, Atmosphere & Health* **2022**, *15*, 1263-1274,doi:10.1007/s11869-021-01141-4.
32. HE, X.; ZHANG, Y.; SUN, B.; WEI, P.; HU, D. Study on Leaf Epidermis Structure and Dust-Retention Ability of Five Machilus Species. *Notulae Botanicae Horti Agrobotanici Cluj-Napoca* **2019**, *47*, 1224-1229, doi:10.15835/nbha47411608.
33. Kretinin, V.M.; Selyanina, Z.M. Dust Retention by Tree and Shrub Leaves and Its Accumulation in Light Chestnut Soils under Forest Shelterbelts. *Eurasian Soil Science* **2006**, *39*, 334-338, doi:10.1134/S1064229306030136.
34. Liu; Guo; Xu; Xiaowu; Hu; Xinghua; Zhao; Jiahao; Lai; Xiaohong; et al. Comprehensive Analysis of the Effect of Stomata on the Retention of Atmospheric Particulates by Plant Leaves. In Proceedings of the

 doi:10.20944/preprints202602.0618.v1



International Conference on Energy and Environmental Science; *Springer*, January 1 2025; pp. 378-393,doi: 10.1007/978-3-032-01036-0_29.

35. Wang, H.; Shi, H.; Li, Y.; Yu, Y.; Zhang, J. Seasonal Variations in Leaf Capturing of Particulate Matter, Surface Wettability and Micromorphology in Urban Tree Species. *Frontiers of Environmental Science & Engineering* **2013**, *7*, 579-588, doi:10.1007/s11783-013-0524-1.
36. Zeybert; EA; Akinshina; NG; Mitusov; AV Dust Retaining Capacity of Deciduous and Coniferous Trees in Tashkent City, *Uzbekistan*. **2022, https://doi.org/10.3390/agriculture15070770**.
37. Kwak, M. J., Lee, J., Park, S., Lim, Y. J., Kim, H., Jeong, S. G., Son, J.-a., Je, S. M., Chang, H., Oh, C.-Y., Kim, K., & Woo, S. Y. (2023). Understanding Particulate Matter Retention and Wash-Off during Rainfall in Relation to Leaf Traits of Urban Forest Tree Species. *Horticulturae*, 9(2), 165. https://doi.org/10.3390/horticulturae9020165
38. Bridhikitti; Arika; Khumphokha; Pawaporn; Wanitha; Wantanan; Prasopsin; Suphat Dust Captured by a Canopy and Individual Leaves of Trees in the Tropical Mixed Deciduous Forest: Magnitude and Influencing Factors. *European Journal of Forest Research* **2024**, *143*, 713-725, https://doi.org/10.1007/s10342-023-01646-w.
39. Sheng, Q., Guo, Y., Lu, J., Song, S., Li, W., Yang, R., & Zhu, Z. (2024). A Study on the Dust Retention Effect of the Vegetation Community in Typical Urban Road Green Spaces—In the Case of Ying Tian Street in Nanjing City. *Sustainability*, 16(7), 2656, https://doi.org/10.3390/su16072656.
40. Gao, Z., Qin, Y., Yang, X., & Chen, B. (2022). PM10 and PM2. 5 Dust-retention capacity and leaf morphological characteristics of landscape tree species in the Northwest of Hebei Province. *Atmosphere*, 13(10), 1657, https://doi.org/10.3390/atmos13101657.
41. Pu, Y. T., Jia, Y. Y., He, M. X., Yao, W. S., Mo, X. Q., & Tao, J. J. (2023). Surface microcosmic structure and dust retention amounts of five evergreen species. In E3S Web of Conferences (Vol. 393, p. 02034). *EDP Sciences*. https://doi.org/10.1051/e3sconf/202339302034
42. Huang; Rong; Tian; Qing; Zhang; Yue; Chen; Zhini; Wu; Yonghua; et al. Differences in Particulate Matter Retention and Leaf Microstructures of 10 Plants in Different Urban Environments in Lanzhou City. *Environmental Science and Pollution Research* **2023**, *30*, 103652-103673, https://doi.org/10.1007/s11356-023-29607-1.
43. Lu, L.; Dongsheng, G.; R., P.M. The Morphological Structure of Leaves and the Dust-Retaining Capability of Afforested Plants in Urban Guangzhou, South China. *Environmental science and pollution research international* **2012**, *19*, null, doi:10.1007/s11356-012-0876-2.
44. Asigbaase; Michael; Dawoe; Evans; Abugre; Simon; Kyereh; Boateng; Nsor, A.; Collins Allometric Relationships between Stem Diameter, Height and Crown Area of Associated Trees of Cocoa Agroforests of Ghana. *Scientific Reports* **2023**, *13*, 14897, https://doi.org/10.1038/s41598-023-42219-6.
45. Tao; Ziwei; Li; Shuxuan; Wang; Bo; Xie; Yi; Wang; Rui; et al. Monitoring Dust Retention Variations in Different Functional Zones Based on Leaf Magnetism and the Influence of Green Belt Spatial Layouts on Leaf Dust Retention. *Environmental Monitoring and Assessment* **2025**, *197*, 360, doi:10.1007/s10661-025-13813-0.
46. Li; Qiaoyun; Liao; Juyang; Zhu; Yingfang; Ye; Zhiqun; Chen; Chan; et al. A Study on the Leaf Retention Capacity and Mechanism of Nine Greening Tree Species in Central Tropical Asia Regarding Various Atmospheric Particulate Matter Values. *Atmosphere* **2024**, *15*, 394, https://doi.org/10.3390/atmos15040394.
47. Xie; Changkun; Guo; Jiankang; Yan; Lubing; Jiang; Ruiyuan; Liang; Anze; et al. The Influence of Plant Morphological Structure Characteristics on PM2. 5 Retention of Leaves under Different Wind Speeds. *Urban Forestry & Urban Greening* **2022**, *71*, 127556, doi:10.1016/j.ufug.2022.127556.
48. Zhang; Zhi; Gong; Jialian; Li; Yu; Zhang; Weikang; Zhang; Tong; et al. Analysis of the Influencing Factors of Atmospheric Particulate Matter Accumulation on Coniferous Species: Measurement Methods, Pollution Level, and Leaf Traits. *Environmental Science and Pollution Research* **2022**, *29*, 62299-62311, doi:10.1007/s11356-022-20067-7.
49. Zeng; Chenlu; Li; Rui; Liao; Yaxuan; Dong; Hao; Liu; Yuxing; et al. Effect of Vacuum Microwave Drying Pretreatment on the Production, Characteristics, and Quality of Jujube Powder. *Lwt* **2025**, *222*, 117674, https://doi.org/10.1016/j.lwt.2025.117674.

 doi:10.20944/preprints202602.0618.v1




50. Yao; Jiaqi; Wu; Shuqi; Cao; Yongqiang; Wei; Jing; Tang; Xinming; et al. Dry Deposition Effect of Urban Green Spaces on Ambient Particulate Matter Pollution in China. *Science of The Total Environment* **2023**, *900*, 165830, https://doi.org/10.1016/j.scitotenv.2023.165830.
51. Wei; Weixuan; Wang; Yiqi; Yan; Qi; Liu; Guanpeng; Dong; Nannan Assessing Buffer Gradient Synergies: Comparing Objective and Subjective Evaluations of Urban Park Ecosystem Services in Century Park, Shanghai. *Land* **2024**, *13*, 1848, https://doi.org/10.3390/land13111848.
52. Sun; Yuqian; Wu; Guangzhao; Li; Pin Evaluation of Ecological Service Functions of Urban Greening Tree Species in Northern China Based on the Species-Specific Air Purification Index. *Forests* **2024**, *15*, 1835, https://doi.org/10.3390/f15101835.
53. Zhang, L., Zhang, X., Yuan, S., & Wang, K. (2021). Economic, Social, and Ecological Impact Evaluation of Traffic Network in Beijing–Tianjin–Hebei Urban Agglomeration Based on the Entropy Weight TOPSIS Method. *Sustainability*, 13(4), 1862. https://doi.org/10.3390/su13041862.
54. Zhang, W., Li, Y., Wang, Q., Zhang, T., Meng, H., Gong, J., & Zhang, Z. (2022). Particulate Matter and Trace Metal Retention Capacities of Six Tree Species: Implications for Improving Urban Air Quality. *Sustainability*, *1*4(20), 13374. https://doi.org/10.3390/su142013374
55. Liu; Xiaocao; Li; Chengzhi; Zhao; Xiaobing; Zhu; Tianyu Arid Urban Green Areas Reimagined: Transforming Landscapes with Native Plants for a Sustainable Future in Aksu, Northwest China. *Sustainability* **2024**, *16*, 1546, https://doi.org/10.3390/su16041546.